

## MECHANISTIC PROTEOMIC PROFILING OF MDR STRAIN EXPOSED TO PLANT-BASED SILVER NANOPARTICLES SYNTHESIZED FROM *BOERHAVIA DIFFUSA*

Sasi Lekha. S<sup>1</sup>, S. Antony<sup>2</sup>

1, Research Scholar, Reg.No: 20113082102008, Department of Microbiology, Malankara Catholic College, Mariagiri, Kaliyakavilai, Affiliated to Manonmaniam Sundaranar University, Tirunelveli, Tamil Nadu, India.

2, Assistant Professor, Department of Microbiology, Malankara Catholic College, Mariagiri, Kaliyakavilai, Affiliated to Manonmaniam Sundaranar University, Tirunelveli, Tamil Nadu, India.

DOI: [https://doi.org/10.63001/tbs.2026.v21.i01.S.l\(1\).pp747-775](https://doi.org/10.63001/tbs.2026.v21.i01.S.l(1).pp747-775)

### KEYWORDS

*Multi Drug Resistance;*  
*B.cereus;*  
*AgNPs;*  
*Two-Dimensional*  
*Electrophoresis;*  
*Mass Spectrometry;*  
*Gene ontology*

Received on: 15-12-2025

Accepted on: 19-01-2026

Published on: 17-03-2026

### ABSTRACT

Biogenic nanoparticles of medicinal plants are an emerging alternative action against multidrug-resistant (MDR) bacteria. *Boerhavia diffusa*, a well-known ethnomedicinal plant, with high phenolic and flavonoid contents, offers an effective reducing and stabilizing agent in the green synthesis of silver nanoparticles (AgNPs). In this study, *B. diffusa* ethanolic extract was used to synthesize AgNPs, and they were characterized to prove the stability and nanoscale properties. The synthesized AgNPs were tested against the MDR strain isolated from pesticide-treated brinjal root soil and were found to have significant inhibitory potential at the effective dose (60 µg). This study aims to determine the effects of the synthesized AgNPs on the proteome of the identified MDR strain (*Bacillus cereus*). Following exposure to the inhibitory concentration of AgNPs (60 µg), intracellular protein was extracted and separated by Two-Dimensional Gel Electrophoresis (2D-GE), which showed specific changes in the intensity of protein spots in treated and control samples. Spots that were differentially expressed on the 2D gels were excised and analyzed by mass spectrometry, which identified 10 proteins that were differentially regulated with AgNP treatment. Gene Ontology (GO) enrichment findings have defined a multi-target cytotoxic pathway in every cellular domain, demonstrating the importance of a systems-level methodology. The Molecular Function (MF) profile showed acute functional distress, highlighted by substantial enrichment in Nucleotide binding and DNA binding. The Biological Process (BP) analysis showed a cell crisis condition, where DNA repair systems became enriched, and Transmembrane transport was severely disturbed. Moreover, the Cellular Component (CC) analysis found the site of damage, the Plasma membrane and Cell envelope were enriched, and structural failure was observed, in addition to the Cytoplasm. The findings prove the multi-targeting character of the AgNPs. In conclusion, the high antibacterial activity exhibited by *B. diffusa*-AgNPs against the MDR strain is supported by proteomic data that reveal the impairment of critical pathways, such as those involved in DNA maintenance, nucleotide synthesis, and membrane bioenergetics. This definitive proteomic evidence validates biogenic AgNPs as a powerful, multi-faceted strategy for combating MDR bacterial pathogenesis.

## 1. INTRODUCTION

The medicinal plants provide an inexpensive, long-term source of bioactive

compounds to address biological issues, especially in treating bacterial infections that

are resistant to medicine (Nikhil *et al.*, 2024). *Boerhavia diffusa* (Punarnava) is especially promising in traditional medicine, mainly owing to its richness in the phenolic acids, flavonoids, and boeravinones, which provide reducing and stabilizing properties that are effective in green nanoparticle assembly (Sudheer *et al.*, 2025). These phytochemicals can not only increase the synthesis but also regulate the biological activity of the nanoparticles made of plants.

Plant-mediated synthetic nanoparticles (AgNPs) of silver have acquired a growing popularity due to their multi-purpose use as antimicrobials and their biocompatibility. Unlike classical antibiotics that usually interfere with only one pathway of cells, AgNPs are characterized by multi-faceted action: harm to membranes, the formation of reactive oxygen species, interference with metabolism, and damage to DNA (Mikhailova *et al.*, 2024). Such a multi-pronged mechanism of action minimizes the possibility of bacteria developing resistance. AgNPs synthesized with medicinal plants are highly effective against MDR pathogens in green synthesis. The AgNPs formed by the *Azadirachta indica* leaf extract showed strong bacterial inhibition against several multidrug-resistant bacteria (Manik *et al.*,

2020). This evidence underscores the potential of plant-derived AgNPs to assist in the fight against the escalating global pandemic of bacterial drug resistance.

AgNPs produced by *B. diffusa* exhibited a high level of inhibition on the MDR strain isolated from pesticide-treated brinjal root soil in this study. These antibacterial effects were particularly striking, but the precise molecular processes underlying the mechanisms of action of AgNPs on disturbing bacterial survival pathways at the proteomic scale are essential to confirm their use as next-generation antimicrobials. Gene Ontology (GO) functional annotation and proteomic profiling are potent and powerful tools to provide an examination of these mechanisms. Through protein expression alterations determined using 2D-GE, and identified differentially regulated proteins using mass spectrometry, and GO-based classification of its proteins, it can be mapped how AgNP exposure disrupts bacterial protein pathways such as DNA repair, ion transport, metabolism, oxidative stress response, and membrane integrity (Liu *et al.*, 2023).

The objective of this study was to synthesize and characterize *B. diffusa*-

mediated AgNPs and examine their mechanistic activity on MDR strains present in pesticide-treated brinjal root soil. Using an integrative proteomic technique such as 2D-GE, Mass spectrometric analysis, and GO functional annotation, it can be determined that the molecular pathways disturbed by AgNPs can give a better understanding of how plant-derived silver nanoparticles execute their antibacterial effect on MDR strains. The knowledge will be helpful in the development of plant-based, non-toxic nanotherapeutics that can address bacterial multidrug resistance.

## 2. Materials and Methods

### 2.1. Synthesis and Characterization of *B. diffusa*-mediated AgNPs

The method proposed by James *et al.* (2015) was used to synthesize AgNPs. 8 mL of ethanolic extract of *B. diffusa* was mixed with 40 mL of the 1 mM AgNO<sub>3</sub> solution. The resulting mixture was incubated at room temperature and shaken at 150 rpm until a dark brown color developed, which indicated the synthesis of nanoparticles. The morphology, elemental composition, and stability of the nanoparticles were determined using UV-Visible spectroscopy, FTIR, FE-SEM, EDAX, XRD, DLS, and TEM.

### 2.2. Assessment of the antibacterial efficacy of silver nanoparticles (AgNPs) against multi-drug resistant (MDR) bacteria isolated from pesticide-treated brinjal root soil

The antimicrobial potential of the synthesized *B. diffusa* AgNPs was tested against the screened MDR isolates using the agar well diffusion method. The MDR isolates were inoculated on nutrient broth, and the cell density was monitored to obtain a 0.5 McFarland turbidity standard. The cultures were swabbed over the MH agar medium, followed by puncturing the medium using a cork borer through which the test samples were assessed for their potential activity. The plates were incubated at 37°C for 24 hours under sterile conditions, and the zone of inhibition was measured in mm (Arul *et al.*, 2017).

### 2.3. Proteomic Analysis of AgNP-treated MDR Isolate

#### 2.3.1. Treatment

The MDR strain (BR-3), which was found to show inhibition on their growth pattern upon *B. diffusa* AgNPs treatment, was sub cultured for 24 hours under controlled conditions and treated with the synthesized AgNPs in the ratio of 50:1 for 24 hrs., along with a control

group – untreated. The treated and untreated bacterial pellets were collected by centrifugation at 6000 rpm for 10 minutes at 4°C.

### 2.3.2. Protein Extraction

The total protein from the untreated and treated *B. cereus* pellets was collected using the TCA precipitation method. The collected untreated and treated pellets were dissolved in PBS and treated with 10% TCA in acetone, having 20mM DTT. The prepared sample was then incubated at -20°C for overnight and then centrifuged at 7800×g for 10 minutes at 4°C. The pellets obtained were washed with acetone twice and then air dried, followed by resolubilization in sample buffer containing 6 M urea, 3 M thiourea, 8% 3-[(cholamidopropyl) dimethylamino]-1-propanesulfonate (CHAPS) (Ananthi *et al.*, 2011).

### 2.3.3. Two-dimensional Gel Electrophoresis

The untreated and treated protein samples were subjected to first dimensional gel electrophoresis followed by rehydration with buffer containing of 7M urea, 2M thiourea, 4% w/v 3-[(3-holamidopropyl/dimethylammonia)-1-propane sulfonate (CHAPS) (Pierce, Rockford, IL, USA), 0.2%

ampholyte 3-10 (Amersham, USA), 100 mM PMSF and 100 mM DTT and focused on rehydrated 13 cm IPG strips (3-10 NL) overnight on IPGphor 2 (GE Healthcare) at a temperature of 20°C at voltage conditions 500 V for 1 hour (step and hold), 1000V for 1 hour (gradient), 8000 V for 3 hour (gradient), and 8000 V for 8 hour (step and hold). The focused strips can be stored at -20°C for long-term storage.

Following which in the second-dimensional electrophoresis the focused strips were equilibrated with equilibration buffer containing 6M Urea, 2M Thiourea, 50 mM Tris, 34.5% Glycerol, 2% SDS, 0.005% bromophenol blue, 2% DTT as reducing agents and 6M Urea, 2M Thiourea, 50 mM Tris, 34.5% Glycerol, 2% SDS, 0.005% bromophenol blue and 2.5% IAA as alkalytic agent in a two-step process.

The strips were then run on a 12.5% polyacrylamide gel, sealed with 0.5% agarose (DALT six apparatus, GE Healthcare) for 30 minutes at 18W and 4.30 h at 50 W at a temperature of 22°C (Ananthi *et al.*, 2018; Sivagnanam *et al.*, 2022). The gels were stained using Coomassie stain (10% phosphoric acid, 10% ammonium sulfate, 0.12% Coomassie Blue G-250, and 20% methanol) overnight and destained

using water to analyse the differentially expressed protein using a gel scanner. All the experimental procedures were performed in duplicates, and the proteins with significant fold change were then identified using the ANOVA (Sivagnanam *et al.*, 2021; Sivagnanam *et al.*, 2022).

#### 2.3.4. In-gel trypsinization

The differentially expressed proteins were then obtained using in-gel trypsinization. The protein spots were excised, destained with 25 mM ammonium bicarbonate in 50% acetonitrile, thrice. The destained spots were dehydrated with 100 % acetonitrile for 15 minutes and dried under vacuum for 30 minutes, followed by trypsin digestion was performed using 400 ng of trypsin (Promega), in 5 $\mu$ l of 100 mM ammonium carbonate and 10% acetonitrile for the incubation period of 30 minutes, after removing excess trypsin the gel spots were soaked with 20 $\mu$ L of 40mM ammonium bicarbonate in 10% acetonitrile and incubated at 37°C water bath for 16 hours. The peptides were then obtained using 25 $\mu$ l of 0.1% trifluoroacetic acid (TFA) made in 60% acetonitrile, through centrifugation followed by sonication for 3 mins at 2200 MHz. The obtained supernatant was

collected and vacuum dried for a time period of 60-90 minutes (Ananthi *et al.*, 2008, 2013).

#### 2.3.5. Mass Spectrometric Analysis

The obtained supernatant was subjected to MALDI-TOF mass spectrometry for the identification of differentially expressed proteins. The  $\alpha$ -cyano-4-hydroxycinnamic acid (CHCA) matrix was prepared at a concentration of 2 mg/ml in 70% acetonitrile and 0.03% trifluoroacetic acid (TFA). A sample volume of 0.7  $\mu$ L was applied over the CHCA matrix on a stainless-steel target plane and identified using the reflector mode with a mass range of 1-5000 Da, at a laser intensity of 35-45 and laser beam diameter of 100 microns, followed by pulsing every 1500 m/z mass. Using the Uniprot database, the output file, and the MASCOT software v. 2.2 (Matrix Science, London, UK), the peptides were identified (Ananthi *et al.*, 2008; Sivagnanam *et al.*, 2022).

### 3. RESULT AND DISCUSSION

#### 3.1. Synthesis and Characterization of *B. diffusa*-mediated AgNPs

Silver nanoparticles (AgNPs) biosynthesis using an ethanolic extract of

*Boerhavia diffusa* was visually validated by a change in color to dark brown after the addition of AgNO<sub>3</sub>, which indicated the reduction of Ag<sup>+</sup> ions to metallic Ag<sup>0</sup> using surface plasmon resonance (SPR) excitation (Fahmy *et al.*, 2019). LC–MS analysis of the extract showed the presence of quercetin, ferulic acid, and caffeic acid as polyphenolic compounds that could donate electrons toward the reduction of metal ions and stabilize the colloid to a hydroxyl and carbonyl interaction (Amini *et al.*, 2019).

UV-Vis spectroscopic assay indicated a strong SPR absorption at 434.80 nm, typical of the spherical AgNPs, which supports the active bioreduction and colloidal stability. A secondary absorbance at 270.32 nm was caused by phenolic compounds in the extract that act as capping agents (Khurana *et al.*, 2021). The lack of absorbance characteristics above 450nm was an indication of high purity and monodispersivity, as was reported in the previous literature (Waychunas *et al.*, 2001). These are findings that align with earlier reports, which state that plant-derived biomolecules mediate nanoparticle growth and prevent aggregation by steric and electrostatic interactions (Edayadulla *et al.*, 2024).

FTIR spectra exhibited major absorption peaks at 3338, 2928, 1652, 1451, 1380, 1086, and 511 cm<sup>-1</sup>, signifying the presence of O–H, C–H, amide, and C–O functional groups, confirming the involvement of phenolics, proteins, and polysaccharides in reduction and capping (Weyer, 2002). EDAX analysis displayed a strong silver signal at 3 keV, with elemental composition of C (42.82%), O (32.16%), and Ag (25.02%), confirming silver as the predominant metallic constituent (Shaik *et al.*, 2018).

FESEM micrographs revealed predominantly spherical, well-dispersed nanoparticles with diameters between 50.28 and 57.78 nm, corroborated by TEM analysis showing spherical to quasi-spherical morphology. The presence of an organic capping layer was evident, while SAED patterns displayed concentric rings confirming polycrystalline, face-centered cubic (fcc) structure (Bamal *et al.*, 2021). XRD peaks at 14.06°, 25.61°, and 27.44° (2θ) corresponded to the (111), (200), and (220) planes of fcc silver, with no impurity peaks, indicating high crystallinity (Poudel *et al.*, 2022).

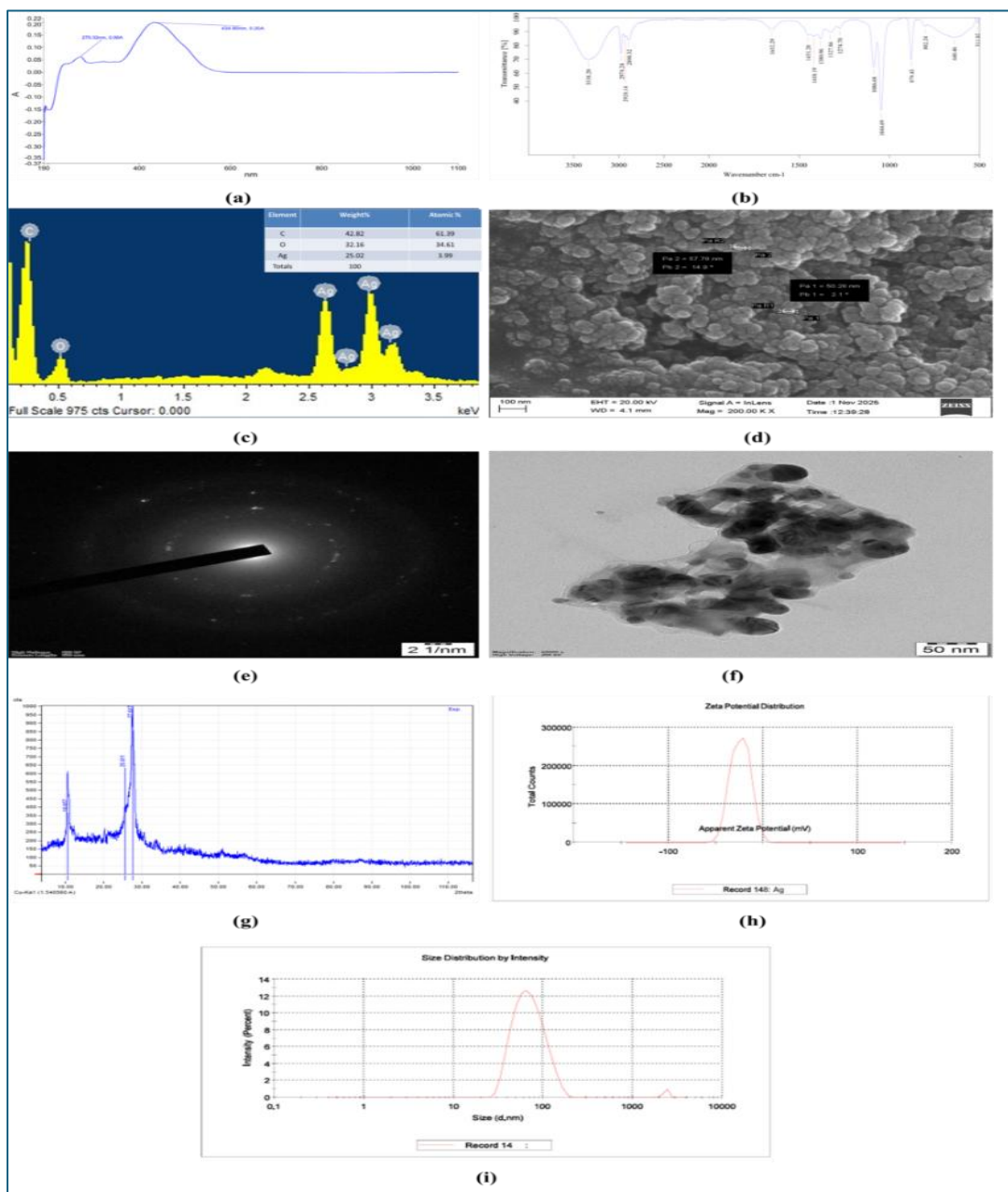


**Fig. 1.** Characterization of *B. diffusa* mediated Silver nanoparticles by (a) UV- Vis Spectrophotometric analysis; (b) FTIR analysis; (c) EDX analysis; (d) FE-SEM; (e) Selected Area Electron Diffraction; (f) TEM analysis; (g) XRD analysis; (h) and (i) DLS analysis

An additional confirmation of the colloidal behavior of *B. diffusa*-derived silver nanoparticles was obtained through dynamic

light scattering (DLS) and zeta potential analyses. The profile of zeta potential (Figure h) reflected a definite peak at around -23.8

mV, which indicates a moderately negative particle surface charge, which facilitates electrostatic stabilization, and lowers the chances of particle aggregation, a trend typical of phytochemical-capped AgNPs (Iravani *et al.*, 2011; Mohammed *et al.*, 2020). In line with this, the DLS intensity distribution (Fig. 1 (i)) showed a dominant hydrostatic diameter of approximately 111 nm with a sharp, unimodal peak, which is in accordance with the monodisperse nature of the nanoparticles expected when plant metabolites were used as natural capping and reducing agents (Ahmed *et al.*, 2016; Raj *et al.*, 2021). This small secondary peak at higher diameters is probably an indication of aggregates, common to biogenic nanoparticles as a result of discontinuous phytochemical surface coverages. Overall, these data support the thesis that *B. diffusa* phytoconstituents enable AgNPs to be assembled with a stable negative charge and a precise distribution of particle sizes, thus justifying their application as a source of antimicrobial and biomedical agents.

### 3.2. Antibacterial Activity of Synthesized AgNPs

The antimicrobial properties of *Boerhavia diffusa*-based silver nanoparticles (AgNPs) against multidrug-resistant (MDR) bacterial strains in pesticide-contaminated brinjal root soil were assessed (Fig.2). The AgNPs showed a unique concentration-dependent inhibitory action, which validates their widespread antibacterial action. High zones of inhibition were observed at 16 mm for (BR3) at a concentration of 60 µg. However, smaller inhibitory zones were noted under the concentrations of 10 µg and 40 µg, respectively. These findings prove that nanoparticle efficacy is dose-dependent alongside improved interactions with nanoparticles and generation of reactive oxygen species (ROS) at higher concentrations (Rai *et al.*, 2012).

The dose-dependent response that was observed in this study agrees with the classical phenomenon of contact-killing, where increased concentration of the nanoparticles provides improved access to the surface and constant release of the silver ions (Agnihotri *et al.*, 2013).

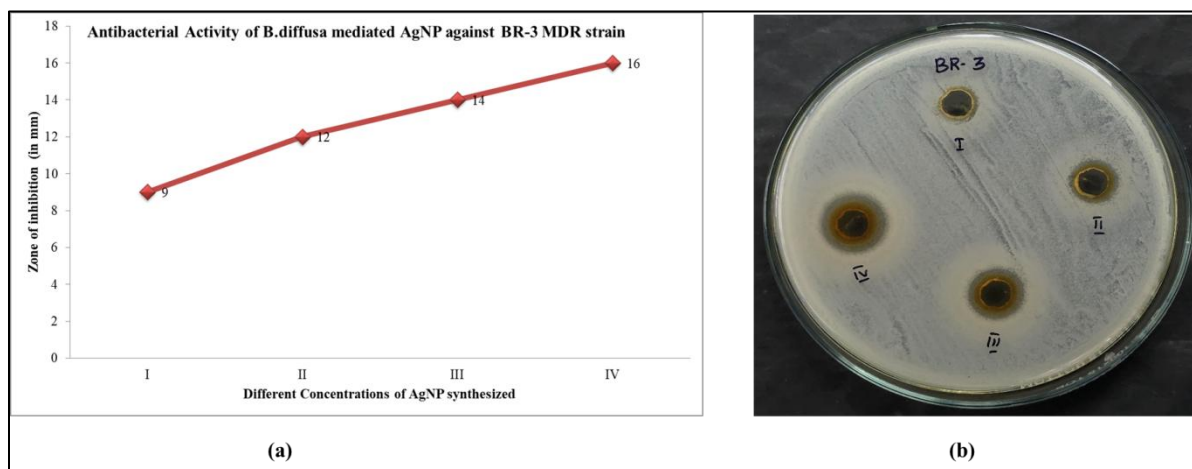


**Fig 2.** Showing the Concentration Dependent Antibacterial Activity of *B. diffusa* Mediated AgNPs against MDR strain (BR-3) from Pesticide Treated Brinjal Root Soil (a) Line graph showing concentration-dependent increase in the zone of inhibition. (b) Agar well diffusion plate displaying inhibition zones at four AgNP concentrations.

\*BR- Code given to the isolates; I-IV correspond to increasing AgNP concentrations of 10, 20, 40, and 60  $\mu\text{g}$ ,

Based on antibacterial efficacy, the MDR strain (BR3) was identified as *B. cereus* by 16S rRNA technique and was chosen for proteomic profiling to explore AgNP-induced changes in protein expression of this MDR strain. The selection of *B. cereus* was particularly significant because it is an environmentally persistent species with strong  $\beta$ -lactam and vancomycin resistance, making it a suitable model for investigating nanoparticle-mediated inhibition of resistance pathways (Ehling-Schulz *et al.*, 2019). Overall, the results confirm that *B. diffusa*-derived AgNPs exert potent antibacterial effects against MDR soil

isolates, validating their potential as eco-friendly antimicrobial agents.

### 3.3. Protein Separation and Quantitative Analysis by Two-Dimensional Gel Electrophoresis

Two-dimensional gel electrophoresis (2D-GE) was used to separate intracellular proteins of both control and *Boerhavia diffusa*-mediated silver nanoparticle (AgNP)-treated cultures of *Bacillus cereus*. The obtained gels contained clear patterns of protein spots, but these patterns were reproducible, which validates the high efficiency of extraction, solubilization, and isoelectric focusing (Fig. 3a- b). The

comparison of the control profile (Fig. 3 (a)) and the treated profile (Fig. 3 (b)) clearly showed that there were significant differences in the spot intensity and

distribution, which implies that the bacterial proteome was altered substantially during the nanoparticle exposure.

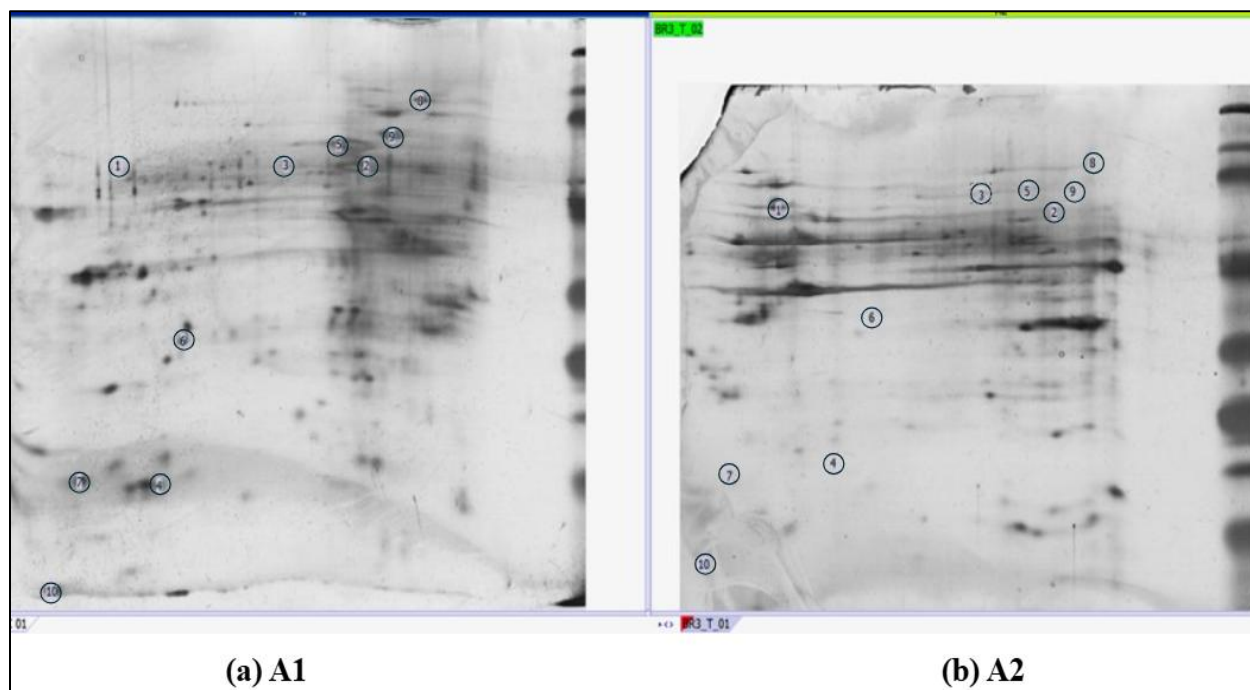


**Fig.3** Representative two-dimensional electrophoresis (2D-GE) maps of *Bacillus cereus* intracellular proteins: (a) A1 Untreated and (b) A2 AgNP-treated.

\* Differentially expressed protein spots are indicated in circles.

Melanie 9.0 software quantitative analysis identified a total of 10 protein spots, which were found to have significant differential expression. Several proteins (spots 2, 3, 4, 5, 6, 7, 8, 9, 10) were significantly downregulated in the treated sample, although one spot (spot 1) was significantly upregulated in comparison with the untreated control. ANOVA statistically confirmed these differences. The numerical

results reported here are in line with the visible decrease of the major protein spots in the treated gels and thus represent the experimental evidence for the AgNPs inhibitory effect on cell protein synthesis and turnover.

The Class Analysis Table provides a summary of the fold-change and level of

significance (p-values) of the differentially expressed proteins.

**Table 1:** Quantitative class analysis of the differentially expressed protein spots in *Bacillus cereus* under control (A1) and *Boerhavia diffusa* AgNP-treated (A2) conditions.

Spot ID	Fold	Anova (p)	A1	A2	Regulation Trend
1	3.29484	0.00412728	2819.75	9290.65	Up regulated
2	2.75199	0.00985007	9693.47	3522.35	Downregulated
3	1.39497	0.0131401	6174.27	4426.1	Downregulated
4	1.532	0.019523	15435.6	10075.5	Downregulated
5	3.36097	0.0287039	19786.7	5887.2	Downregulated
6	4.30893	0.0395415	25757.8	5977.78	Downregulated
7	3.35094	0.0465828	51561.7	15387.2	Downregulated
8	3.53727	0.0473549	20088.7	5679.15	Downregulated
9	3.63324	0.0562188	18807.1	5176.4	Downregulated
10	4.9322	0.0573363	72512.4	14701.8	Downregulated

\*A1: Control (untreated); A2: *B. diffusa*-synthesized AgNPs treated.; Fold Change is the relative change in spot intensity. The values of Expression Ratio <1.0 display down-regulation; the values of Expression Ratio >1.0 display up-regulation.

In addition, the Expression Analysis Table offers normalized intensity ratios between the untreated (A1) and AgNP-treated (A2) samples. An intensive decrease in the spot intensity was also found in the treated cells, which demonstrates the oxidative and translational stress (Table 2).

**Table 2:** Quantitative expression analysis of the differentially expressed protein spots in *Bacillus cereus* under control (A1) and *Boerhavia diffusa* AgNP-treated (A2) conditions.

Spot ID	A1	A2
1	1	3.29484
2	1	0.363374
3	1	0.716863
4	1	0.652742
5	1	0.297533

6	1	0.232076
7	1	0.298424
8	1	0.282704
9	1	0.275236
10	1	0.202749

\*A1: Control (untreated); A2: *B. diffusa*-synthesized AgNPs treated.

The decrease in total spot intensity is consistent with the past literature showing that AgNPs can cause protein oxidation, aggregation, and degradation through the formation of reactive oxygen species (ROS) and reacting with the thiol amino groups of the enzymes (Barros *et al.*, 2019; Mao *et al.*, 2016). This selective up-regulation of c-specific proteins can be taken as an indication of the activation of adaptive defense, such as antioxidant and repair pathways, activated by exposure to nanoparticles (Zhang *et al.*, 2020).

In this way, the 2D-GE profile provides the first indication that alterations in key cellular mechanisms, including metabolic regulation, stress-response pathways, and protein turnover in *B. cereus*, accompany the antibacterial inhibition caused by *B. diffusa*-synthesized AgNPs. The presence of a low metabolic protein concentration and elevated stress-related

proteins suggests that oxidative stress, as well as ionic imbalances, are the key to the antibacterial effect of biogenic AgNPs. The differentially expressed protein spots were then identified by MALDI-TOF/TOF mass spectrometry to characterize their functions.

### 3.4. Identification of Differently Expressed Protein by Mass Spectrometry

Mass spectrometric identification of MALDI-TOF/TOF peptide mass fingerprinting indicated 10 proteins that have significant differences in their expression between *Bacillus cereus* treated with AgNP and untreated control (Table 3). The differentially expressed proteins were observed to be involved in a wide range of cellular events, including RNA metabolism, energy generation, ion transport, and oxidative stress response, indicating a general adaptive response to the stress caused by nanoparticles.

**Table 3:** Differentially expressed proteins identified in *Bacillus cereus* by Mass Spectrometric Analysis

Spot ID	Accession #	Gene ID	Protein Name	Score	Coverage	Mol Weight	pI
1	PNP_BACCN	pnp	Polyribonucleotide nucleotidyltransferase	52	8	78.341	5.08
2	PHLD_BACCE	cerA	Phospholipase C	53	20	32.353	7.1
3	SECA_BACC1	secA	Protein translocase subunit SecA	103	24	95.252	5.43
4	IXTPA_BACCZ	-	dITP/XTP pyrophosphatase	43	27	23.323	4.9
5	PURL_BACC4	purL	Phosphoribosyl Formylglycinamide synthase subunit PurL	51	18	80.711	4.89
6	GERN_BACCE	gerN	Na (+) /H (+) -K (+) antiporter GerN	42	8	41.237	5.96
7	FOSB_BACCE	fosB	Metallothiol transferase FosB	70	73	16.497	6.07
8	ADDB_BACC1	addB	ATP-dependent helicase/deoxyribonuclease subunit B	54	15	134.758	5.38

9	MUTS2_BACC 2	mutS2	Endonuclease MutS2	63	22	88.511	5.89
10	HIS2_BACCZ	hisE	Phosphoribosyl-ATP pyrophosphatase	56	37	12.571	4.98

The identified proteins had a molecular mass of 12.5 kDa to 134.7 kDa, with an isoelectric point of 4.8 to 7.1. Out of the ten proteins identified, Polyribonucleotide nucleotidyltransferase (PNPase) (Spot 1) was upregulated, and the remaining 9 proteins were downregulated as a result of AgNP treatment.

Spot 1 was found to be upregulated by 3.29-fold, and those were identified to be Polyribonucleotide Nucleotidyltransferase (PNPase). The upregulation of Polyribonucleotide Nucleotidyltransferase (PNPase) implies the expression of an adaptive stress response linked to damage caused by nanoparticles. PNPase is a versatile RNA-processing enzyme that is an essential component of mRNA turnover, mRNA degradation, and post-transcriptional regulation, particularly during environmental or oxidative stress (Barria *et al.*, 2016). Its high expression levels in AgNP-treated cells suggest that *B. cereus* is trying to eliminate oxidatively damaged RNA molecules and restructure its transcriptome to improve

survival under nanoparticle stress. PNPase upregulation is an indicator of a compensatory process that reduces RNA oxidation and preserves transcript quality (Briani *et al.*, 2016). The same findings were reported in bacteria exposed to heavy metals and oxidants, where high PNPase activity facilitates RNA quality control and the selective stabilisation of stress-associated transcripts (Vargas-Blanco *et al.*, 2020). The upregulation of PNPase can also destabilize the transcriptome by breaking down critical mRNAs, thereby increasing the metabolic imbalance and cell death (Pizzoccheri *et al.*, 2025).

Multiple essential proteins involved in metabolism, secretion, and detoxification

were markedly downregulated in the present study. Phospholipase C (PLC) is a biologically active molecule that is membrane-bound and depends on phospholipids for its activity. It plays a significant role in altering the membrane, producing toxins, increasing virulence, and regulating signal transduction (Singh *et al.*, 2023). In the current study, *B. cereus* treated with AgNPs showed a significant downregulation of PLC, suggesting that membrane lipid metabolism and signaling pathways were affected. This alteration most certainly changes the membrane from the inside and out, thereby permeabilizing; cellular leakage ensues, and pathogenic potential is reduced. Monturiol-Gross *et al.* (2021) report similar findings in their study that bacterial virulence and host-cell invasion are greatly affected when PLC is inhibited. The downregulation of PLC is linked to the antibacterial effect of AgNPs, as described earlier, in which the nanoparticles get involved with bacterial membranes, causing oxidative stress and lipid bilayer structural disintegration, thus leading to oxidative membrane damage (Terehova *et al.*, 2021; More *et al.*, 2023).

The downregulation of SecA is an indication that AgNPs disrupt the bacterial

secretory apparatus, thus hindering the export of vital proteins to assemble cell walls, uptake nutrients, and secret virulence factors. SecA in *Bacillus cereus* is an ATPase motor protein that enables the precursor proteins to cross the SecYEG channel during post-translational translocation (Tsirigotaki *et al.*, 2017). Previous studies have shown that silver nanoparticles can bind to membrane-associated proteins and prevent ATP-dependent enzymatic reactions, failing to translocate proteins and accumulate precursor proteins in the cytoplasm (Dakal *et al.*, 2016). Moreover, the morphological and physiological damage to the cells being treated may also be linked to downregulation of the SecA, which is essential in the retention of membrane integrity and cell viability by the Sec pathway. Inability to export stress-response proteins and enzymes required to synthesize peptidoglycan can make the bacterium more vulnerable to oxidative stress and lysis caused by nanoparticles (Kashyap *et al.*, 2014). Thus, the inhibition of SecA expression that has been observed shows that *B. diffusa*-mediated AgNPs can inhibit the bacterial protein translocation system, affecting essential housekeeping and virulence-associated pathways to support cell survival.

Likewise, the observed downregulation of dITP/XTP pyrophosphatase suggests that exposure to AgNPs modifies bacterial purine metabolism and DNA repair processes. In this case, downregulation of dITP/XTP pyrophosphatase may result in the proliferation of noncanonical nucleotides in the cytoplasm, which can promote mutagenesis, transcriptional errors, and disrupted DNA replication (Davies *et al.*, 2011). A decrease in the amount of expressed enzyme can also indicate an absence of nanoparticles interfering with metal-binding motifs and ATP-dependent catalytic enzyme domains. Numerous bacterial pyrophosphatases require  $Mg^{2+}$  or  $Mn^{2+}$  cofactors, and  $Ag^+$  ions can replace them, causing conformational destabilization and loss of catalytic activity (Zyryanov *et al.*, 2002). In addition, the oxidative alteration of the active-site cysteine and histidine residues by radicals produced by AgNPs may further inhibit enzymatic turnover (Liu *et al.*, 2020). Simultaneous loss of membrane integrity, ROS formation, and failure of nucleotide sanitation are likely to be synergic to induce cell death in *B. cereus*.

Phosphoribosyl  
Formylglycinamylglycinamide synthase

subunit PurL catalyzes an essential step in the de novo purine biosynthetic pathway to the generation of inosine monophosphate (IMP) (Ebbole *et al.*, 1987). The significant reduction of purL in the AgNP-treated cells points to the high inhibition of nucleotide metabolism, which leads to the lack of purine precursors to synthesise DNA and RNA. AgNPs have been found to induce a similar repression of purine biosynthetic genes in *E. coli* and *Staphylococcus aureus*, indicating a change in anabolic processes to their energy-saving stress responses (Saulou-Berion *et al.*, 2015; Singh *et al.*, 2019). As purL mutations in *Bacillus* species cause growth defects and purine auxotrophy (Xia *et al.*, 2011), the decrease in PurL concentration might also play a role in causing the growth and viability deficiencies of the AgNP-treated cultures. The observation highlights the fact that AgNP toxicity is not only confined to membrane damage, but it also involves disruption of the key biosynthetic pathways involved in replication and the survival of the cell mass (Mao *et al.*, 2016).

After this metabolic inhibition,  $Na^+/H^+-K^+$  antiporter GerN, a membrane protein that supports ionic and osmotic homeostasis in *Bacillus*, was also significantly downregulated (Southworth *et*

*al.*, 2001). The inhibition of GerN indicates that AgNPs inhibit ion transport and proton motive force (PMF), resulting in acidification of the cytoplasm and loss of electrochemical gradients. It has been reported that AgNPs inhibit ion exchange and ATP production by binding thiol and replacing metal cofactors like  $Mg^{2+}$  or  $Fe^{2+}$  (Silver, 1996; Kawish *et al.*, 2020). This causes depolarisation, leakage of critical ions, and has been observed in nanoparticle-treated *E. coli* and *S. aureus* with PMF collapse preclinically followed by cell death (Molina-Hernandez *et al.*, 2021). In that way, the downregulated GerN highlights the fact that AgNPs directly attack bacterial membrane bioenergetics to damage homeostasis and viability of bacteria.

Together, the Metallothioltransferase FosB, which is commonly used to counteract electrophilic stress elements, including the antibiotic fosfomycin, was significantly suppressed in the treated samples. FosB enzyme catalyses the conjugation of bacillithiol or L-cysteine to the epoxide ring of fosfomycin, which is one of the critical reactions to oxidative and antibiotic stress in bacteria (Cao *et al.*, 2001). Its down-regulation means that AgNPs repress natural detoxification pathways, presumably by oxidative inactivation of thiol and metal-

binding residues (Helmann *et al.*, 2011; Cameron *et al.*, 2022). The resulting impairment of the detoxification ability exposes cells to increased risk of oxidative damage and accumulation of ROS, which exacerbates the toxicity of nanoparticles. It was also found that comparable decreases in FosB and antioxidant enzymes occur when Gram-positive bacteria are treated with metal nanoparticles (Hsueh *et al.*, 2015; Li *et al.*, 2021), which supports evidence that AgNPs enhance bactericidal activity by disabling redox regulation and stress resistance systems simultaneously.

The proteomic study revealed a considerable downregulation in the ATP-dependent helicase/deoxyribonuclease subunit B, which is an enzyme that is necessary in DNA replication, recombination, and repair indicating that AgNP exposure compromises the bacterial DNA maintenance machinery, thereby contributing directly to their antibacterial effect (Handtke *et al.*, 2018). This downregulation of this helicase may indicate that AgNPs disrupt the DNA maintenance apparatus of *B. cereus*, perhaps by reacting with the metal cofactors or catalytic residues constituting ATP hydrolysis (Doly *et al.*, 1978). This kind of inhibition may lead to stalling of the

replication fork and accumulation of the double-strand break, which causes genomic instability (Ayora *et al.*, 2011). Furthermore, a downregulation of helicase could indicate a metabolic switching of energy sources to antioxidant defences instead of replication in extreme oxidative situations (Ezraty *et al.*, 2017). Irrespective of the mechanism, the inhibition of this enzyme impairs the integrity of the genome, which ultimately leads to a decrease in the survival of bacteria.

In line with this, the endonuclease MutS2 that facilitates the processes of homologous recombination and ribosome rescue (Fukui *et al.*, 2007) was also significantly decreased. MutS2 has a small MutS-related (Smr) domain, which allows endonucleolytic dissolving of the stalled translation complex and the recombination intermediate. Downregulation of this enzyme suggests that AgNPs affect the process of DNA repair and quality control during translation, resulting in the presence of ribosomal collisions and non-complete transcripts (Park *et al.*, 2024). Oxidative stress induced by silver ions must probably remove key cofactors of the MutS2 active Site, disrupting its activity (Flores-Lopez *et*

*al.*, 2019). As a result, *B. cereus* cells subjected to AgNPs show less ability to repair replication errors and canonical translation errors, leading to faster accumulation of cell death.

The upregulation of stress-related nucleic acid processing proteins and a downregulation of energy and transport proteins indicate a bipolar response in bacteria. This reaction is a sign of attempting to repair damages and, at the same time, a metabolic shutdown reaction in order to maintain cell integrity. Such transition eventually results in the prevention of bacterial multiplication and may cause cell death, which validates the high antimicrobial action of silver nanoparticles (AgNPs) (Bruna *et al.*, 2021).

### 3.5. Gene Ontology (GO) Functional Classification

Gene ontology (GO) analysis of the differentially expressed proteins (DEPs) of *Bacillus cereus* exposed to *Boerhavia diffusa*-mediated silver nanoparticles (AgNPs) offered abundant information on the functional and mechanistic roles of the proteins, at the molecular, biological, and cellular levels (Fig. 4a- c).

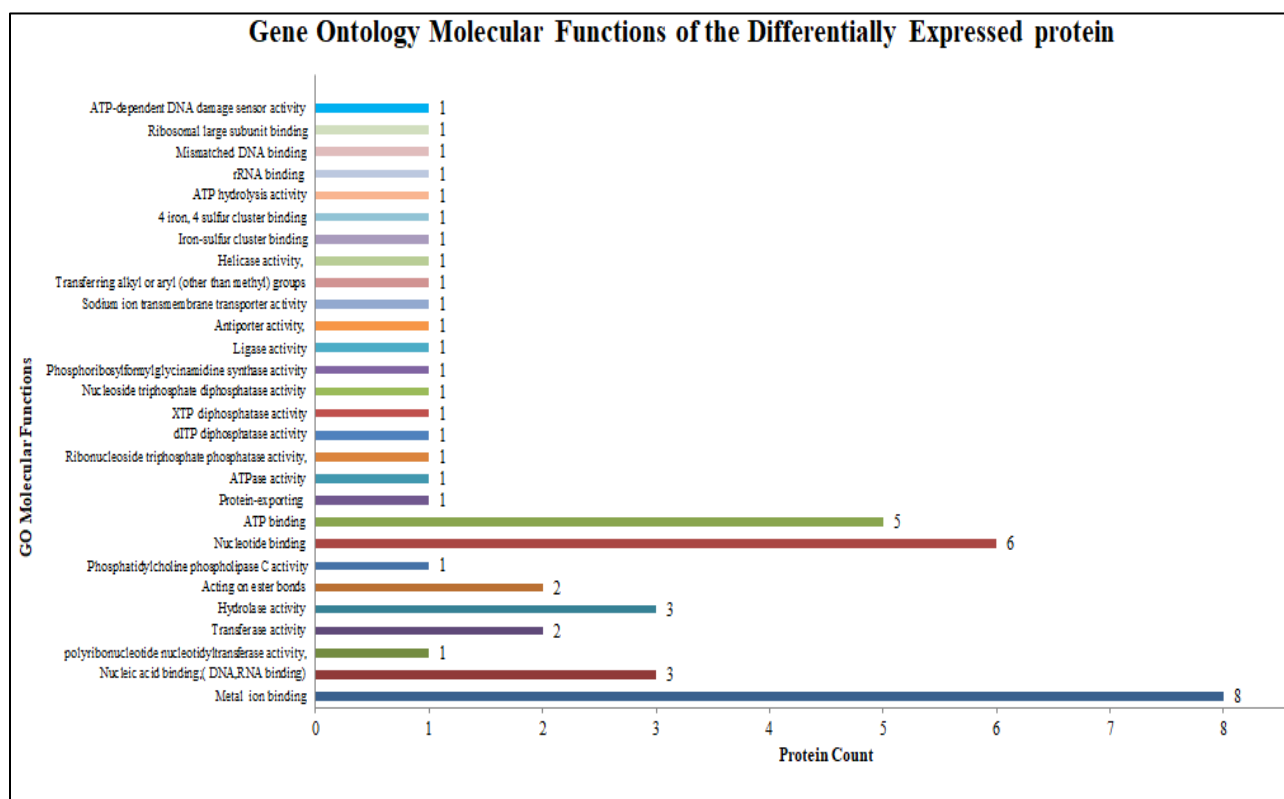


**Fig. 4 (a) Gene Ontology (GO) analysis representing the molecular functions of differentially expressed proteins**

As shown in the analysis, most of the proteins have been functionally linked to metal ion binding, nucleotide binding, and ATP binding, which indicates their role in the maintenance of ionic balance and energy metabolism in the cell under stress. Metal ion-binding protein enrichment proposes that they play a pivotal role in oxidative homeostasis and stabilisation of oxidative metalloenzymes, required to catalyse and transfer electrons in oxidative stress reactions. Similarly, the elevation of nucleic acid-binding and ATP-dependent proteins means

an active role in DNA repair, replication, and transcriptional regulation, which helps in the maintenance of the integrity of the genome and metabolic stability in nanoparticle exposure. These results can be compared with the earlier works in proteomics, which have proved the interaction of ATP- and DNA-binding proteins to support stressful situations and allow bacteria to survive via amplified DNA repair and redoxing processes (Ayora *et al.*, 2011; Ezarty *et al.*, 2017).

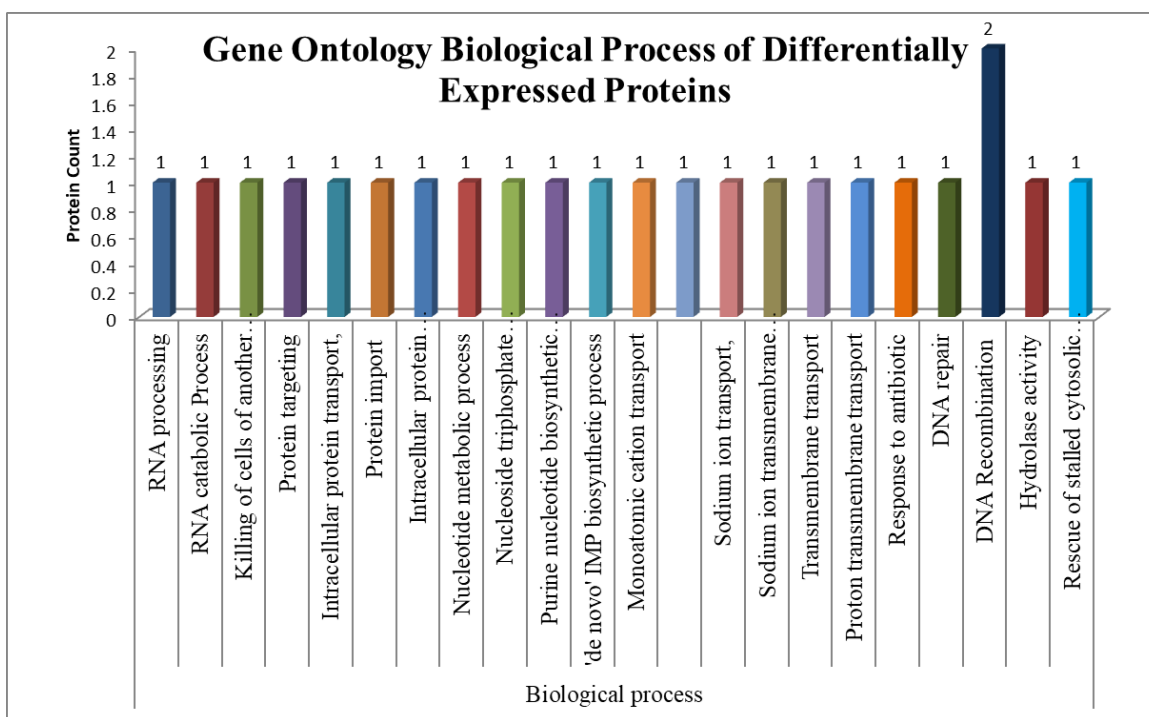


**Fig. 4 (b) Gene Ontology (GO) analysis representing the biological processes associated with differentially expressed proteins**

Biological process ontology showed substantial enrichment in proteins relating to transmembrane transport, protein trafficking, and nucleoside metabolic pathways (Fig. 4b). The presence of proteins associated with DNA repair, RNA processing, and response to metabolic stress was also observed, which indicates a cell reprogramming of homeostasis to survive in oxidative conditions created by nanoparticles. The increased expression of transport-related proteins, especially ion translocation and membrane trafficking, is associated with an adaptive approach to osmotic homeostasis, as well as to the regulation of efflux of toxic

intermediates. These mechanisms are essential for the survival of bacteria, and they were found in a microorganism under stress, implying a primary response of the organism to the exposure to metal nanoparticles (Hassan *et al.*, 2017; Pal *et al.*, 2022). The expression and presence of DNA recombination proteins, as well as RNA processing proteins, demonstrate the presence of an integrated response allowing a quick adjustment of gene expression, leading to resilience against oxidative and metabolic stress. Mechanistically, the responses could be mediated by ATP-dependent proteins and the SOS regulatory domain that jointly

organise the process of DNA repair and protein quality management in unfavorable conditions (Maslowska *et al.*, 2019).

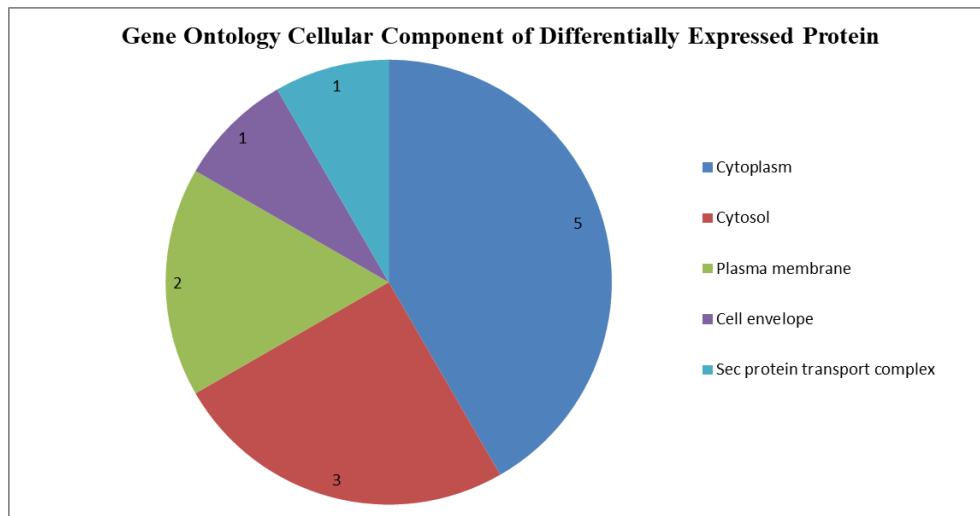


**Fig 4 (c).** Gene Ontology (GO) analysis represents the cellular components of differentially expressed proteins.

The cellular component analysis revealed a primary cell localization of proteins in the cytoplasm and cytosol, followed by the plasma membrane, cell envelope, and then the Sec protein transport complex. The preeminence of cytoplasmic and membrane-bound proteins highlights their role in cell defense, metabolism, and stress signaling. The membrane-bound proteins, associated with the Sec translocation system, are essential to protein secretion, environmental communication, and envelope integrity maintenance during metal stress (Stephenson *et al.*, 2005). This pattern of spatial distribution indicates a coordinated cellular

approach in which metabolic enzymes, structural proteins, and transporters collaborate to oppose nanoparticle-induced disruption of redox balance and membrane permeability of the cell.

In general, the GO enrichment analysis helps to demonstrate that *B. cereus* reacts to AgNP treatment mediated by *B. diffusa* by the activation of functional categories associated with energy metabolism, macromolecular repair, and stress tolerance. The combination of the molecular activities of the ATP-binding proteins and metal ions, and biological mechanisms of transmembrane

transportation and nucleoside metabolism, demonstrates that the bacteria experience an adaptive change in metabolic activity to withstand the oxidative stress exerted by nanoparticles. Such alterations can be linked to previous studies that described bacterial cells as altering their proteomic networks to boost DNA repair, antioxidant protection, and energy production in response to exposure to nanoparticles or other environmental stressors (Barros *et al.*, 2019; Munir *et al.*, 2023). The combination of the GO profiling of the redox-active enzymes, membrane-bound transporters, and nucleic acid-binding proteins leads to the cellular resilience and survival of the *B. cereus* in the presence of the AgNPs.

## CONCLUSION

The present study presents clear proteomic findings that confirm that a decisive two-pronged mechanism describes the strong antimicrobial effect of biogenic *B. diffusa*-AgnPs on MDR *Bacillus cereus* from pesticide treated Brinjal root soil. Protein extraction was carried out for the Minimum inhibitory concentration of AgNP-treated *B. cereus*, followed by 2D gel Electrophoresis, which resulted in 10 differentially expressed proteins, followed by mass spectrometric analysis. The results of this Gene Ontology

analysis validate that the nanoparticles cause concomitant destruction of Cellular Integrity at the plasma membrane, which causes the failure of transport, and trigger genomic Collapse by causing high enrichment of DNA-binding and DNA-repair pathways. This multi-target simultaneous attack destroys the defense mechanisms of the bacteria, which makes AgnPs a special network compared to classic single-target antibiotics. In this work, *B. diffusa*-AgnPs have not only been confirmed as a high-efficiency therapeutic agent, but have also presented the exact molecular template, which can be utilized to design the future approach toward addressing the urgent threat of hyper-resistance associated with multidrug resistance.

## REFERENCE

1. Woolhouse M, Ward M, Van Bunnik B, Farrar J. Antimicrobial resistance in humans, livestock and the wider environment. Philosophical Transactions of the Royal Society B: Biological Sciences. 2015 Jun 5;370(1670):20140083. <https://doi.org/10.1098/rstb.2014.0083>

2. Hassan KA, Fagerlund A, Elbourne LD, Vörös A, Kroeger JK, Simm R, Tourasse NJ, Finke S, Henderson PJ, Økstad OA, Paulsen IT. The putative drug efflux systems of the *Bacillus cereus* group. *PloS one*. 2017 May 4;12(5):e0176188.  
<https://doi.org/10.1371/journal.pone.0176188>
3. Dakal TC, Kumar A, Majumdar RS, Yadav V. Mechanistic basis of antimicrobial actions of silver nanoparticles. *Frontiers in microbiology*. 2016 Nov 16;7:1831.  
<https://doi.org/10.3389/fmicb.2016.01831>
4. More PR, Pandit S, Filippis AD, Franci G, Mijakovic I, Galdiero M. Silver nanoparticles: bactericidal and mechanistic approach against drug-resistant pathogens. *Microorganisms*. 2023 Feb 1;11(2):369.  
<https://doi.org/10.3390/microorganisms11020369>
5. Eker F, Akdaşçi E, Duman H, Bechelany M, Karav S. Green synthesis of silver nanoparticles using plant extracts: A comprehensive review of physicochemical properties and multifunctional applications. *International Journal of Molecular Sciences*. 2025 Jun 27;26(13):6222.  
<https://doi.org/10.3390/ijms26136222>
6. Zheng X, Wang J, Chen Y, Wei Y. Comprehensive analysis of transcriptional and proteomic profiling reveals silver nanoparticles-induced toxicity to bacterial denitrification. *Journal of Hazardous Materials*. 2018 Feb 15;344:291-8.  
<https://doi.org/10.1016/j.jhazmat.2017.10.028>
7. Kumar PV, Pammi SV, Kollu P, Satyanarayana KV, Shameem U. Green synthesis and characterization of silver nanoparticles using *Boerhaavia diffusa* plant extract and their antibacterial activity. *Industrial Crops and Products*. 2014 Jan 1;52:562-6.  
<https://doi.org/10.1016/j.indcrop.2013.10.050>
8. Bauer AW, Kirby WM, Sherris JC, Turck M. Antibiotic susceptibility testing by a standardized single disk method. *American journal of clinical pathology*. 1966 Apr 1;45(4\_ts):493-6.  
[https://doi.org/10.1093/ajcp/45.4\\_ts.493](https://doi.org/10.1093/ajcp/45.4_ts.493)
9. Ananthi S, Santhosh RS, Nila MV, Prajna NV, Lalitha P, Dharmalingam K. Comparative proteomics of human male and female tears by two-dimensional electrophoresis. *Experimental eye research*. 2011 Jun 1;92(6):454-63.  
<https://doi.org/10.1016/j.exer.2011.03.002>
10. Ananthi S, Lakshmi CN, Atmika P, Anbarasu K, Mahalingam S. Global quantitative proteomics reveal deregulation of cytoskeletal and apoptotic signalling proteins in oral tongue squamous cell carcinoma. *Scientific Reports*. 2018 Jan 25;8(1):1567.  
<https://doi.org/10.1038/s41598-018-19937-3>
11. Sivagnanam A, Shyamsundar V, Kesavan P, Krishnamurthy A, Thangaraj SV, Venugopal DC, Kasirajan H, Ramani P, Sarma VR, Ramshankar V. 2D-DIGE-Based Proteomic Profiling with Validations Identifies Vimentin as a Secretory

- Biomarker Useful for Early Detection and Poor Prognosis in Oral Cancers. *Journal of Oncology*. 2022;2022(1):4215097. <https://doi.org/10.1155/2022/4215097>
12. Sivagnanam A, Shyamsundar V, Krishnamurthy A, Thangaraj SV, Srinivas CD, Kasirajan H, Ramani P, RAMSHANKAR V. Evaluation of Vimentin as a Potential Poor Prognostic Indicator and Salivary Biomarker for Oral Cancers and Pre-Cancers by Mass Spectrometry Based Proteomics. <https://doi.org/10.21203/rs.3.rs-656555/v1>
  13. Ananthi S, Chitra T, Bini R, Prajna NV, Lalitha P, Dharmalingam K. Comparative analysis of the tear protein profile in mycotic keratitis patients. *Molecular Vision*. 2008 Mar 12;14:500.
  14. Ananthi S, Venkatesh Prajna N, Lalitha P, Valarnila M, Dharmalingam K. Pathogen induced changes in the protein profile of human tears from Fusarium keratitis patients. *PLoS One*. 2013 Jan 8;8(1):e53018. <https://doi.org/10.1371/journal.pone.0053018>
  15. Fahmy HM, Mosleh AM, Abd Elghany A, Shams-Eldin E, Serea ES, Ali SA, Shalan AE. Coated silver nanoparticles: Synthesis, cytotoxicity, and optical properties. *RSC advances*. 2019;9(35):20118-36. <https://doi.org/10.1039/C9RA02907A>
  16. Amini SM, Akbari A. Metal nanoparticles synthesis through natural phenolic acids. *IET nanobiotechnology*. 2019 Oct;13(8):771-7. <https://doi.org/10.1049/iet-nbt.2018.5386>
  17. Khurana K, Jaggi N. Localized surface plasmonic properties of Au and Ag nanoparticles for sensors: a review. *Plasmonics*. 2021 Aug;16(4):981-99. <https://doi.org/10.1007/s11468-021-01381-1>
  18. Waychunas GA. Structure, aggregation and characterization of nanoparticles. *Reviews in Mineralogy and geochemistry*. 2001 Jan 1;44(1):105-66. <https://doi.org/10.2138/rmg.2001.44.04>
  19. Edayadulla N, Sundari CS. Role of stabilizing agent role in nanomaterials (NM). In *Sustainable Green Synthesised Nano-Dimensional Materials for Energy and Environmental Applications 2024* Dec 5 (pp. 47-63). CRC Press.
  20. Shaik MR, Khan M, Kuniyil M, Al-Warthan A, Alkathlan HZ, Siddiqui MR, Shaik JP, Ahamed A, Mahmood A, Khan M, Adil SF. Plant-extract-assisted green synthesis of silver nanoparticles using *Origanum vulgare* L. extract and their microbicidal activities. *Sustainability*. 2018 Mar 22;10(4):913. <https://doi.org/10.3390/molecules22010165>
  21. Poudel DK, Niraula P, Aryal H, Budhathoki B, Phuyal S, Marahatha R, Subedi K. Plant-Mediated Green Synthesis of Ag NPs and Their Possible Applications: A Critical Review. *Journal of Nanotechnology*. 2022;2022(1):2779237. <https://doi.org/10.1155/2022/2779237>

22. Iravani S. Green synthesis of metal nanoparticles using plants. *Green chemistry*. 2011;13(10):2638-50. <https://doi.org/10.1039/C1GC15386B>
23. Mohammed AA, Al-Musawi TJ, Kareem SL, Zarrabi M, Al-Ma'abreh AM. Simultaneous adsorption of tetracycline, amoxicillin, and ciprofloxacin by pistachio shell powder coated with zinc oxide nanoparticles. *Arabian Journal of Chemistry*. 2020 Mar 1;13(3):4629-43. <https://doi.org/10.1016/j.arabjc.2019.10.010>
24. Ahmed S, Ahmad M, Swami BL, Ikram S. Green synthesis of silver nanoparticles using *Azadirachta indica* aqueous leaf extract. *Journal of radiation research and applied sciences*. 2016 Jan 1;9(1):1-7. <https://doi.org/10.1016/j.jrras.2015.06.006>
25. Raj S, Trivedi R, Soni V. Biogenic synthesis of silver nanoparticles, characterization and their applications—a review. *Surfaces*. 2021 Dec 31;5(1):67-90. <https://doi.org/10.3390/surfaces501003>
26. Iravani S. Green synthesis of metal nanoparticles using plants. *Green chemistry*. 2011;13(10):2638-50. <https://doi.org/10.1039/C1GC15386B>
27. Mohammed AA, Al-Musawi TJ, Kareem SL, Zarrabi M, Al-Ma'abreh AM. Simultaneous adsorption of tetracycline, amoxicillin, and ciprofloxacin by pistachio shell powder coated with zinc oxide nanoparticles. *Arabian Journal of Chemistry*. 2020 Mar 1;13(3):4629-43. <https://doi.org/10.1016/j.arabjc.2019.10.010>
28. Ahmed S, Ahmad M, Swami BL, Ikram S. Green synthesis of silver nanoparticles using *Azadirachta indica* aqueous leaf extract. *Journal of radiation research and applied sciences*. 2016 Jan 1;9(1):1-7. <https://doi.org/10.1016/j.jrras.2015.06.006>
29. Raj S, Trivedi R, Soni V. Biogenic synthesis of silver nanoparticles, characterization and their applications—a review. *Surfaces*. 2021 Dec 31;5(1):67-90. <https://doi.org/10.3390/surfaces501003>
30. Agnihotri S, Mukherji S, Mukherji S. Immobilized silver nanoparticles enhance contact killing and show highest efficacy: elucidation of the mechanism of bactericidal action of silver. *Nanoscale*. 2013;5(16):7328-40. <https://doi.org/10.1039/C3NR00024A>
31. Barros D, Pradhan A, Mendes VM, Manadas B, Santos PM, Pascoal C, Cássio F. Proteomics and antioxidant enzymes reveal different mechanisms of toxicity induced by ionic and nanoparticulate silver in bacteria. *Environmental Science: Nano*. 2019;6(4):1207-18. <https://doi.org/10.1039/C8EN01067F>
32. Mao BH, Tsai JC, Chen CW, Yan SJ, Wang YJ. Mechanisms of silver nanoparticle-induced toxicity and important role of autophagy. *Nanotoxicology*. 2016 Sep 13;10(8):1021-40. <https://doi.org/10.1080/17435390.2016.1189614>

33. Zhang Y, Pan X, Liao S, Jiang C, Wang L, Tang Y, Wu G, Dai G, Chen L (2020) Quantitative proteomics reveals the mechanism of silver nanoparticles against multidrug-resistant *Pseudomonas aeruginosa* biofilms. *J Proteome Res* 19(8):3109–3122.  
<https://doi.org/10.1021/acs.jproteome.0c00114>
34. Bárria C, Pobre V, Bravo AM, Arraiano CM. Ribonucleases as modulators of bacterial stress response. *Stress and Environmental Regulation of Gene Expression and Adaptation in Bacteria*. 2016 Aug 26:174-84.  
<https://doi.org/10.1002/9781119004813.ch14>
35. Briani F, Carzaniga T, Dehò G. Regulation and functions of bacterial PNPase. *Wiley Interdisciplinary Reviews: RNA*. 2016 Mar;7(2):241-58.  
<https://doi.org/10.1002/wrna.1328>
36. Vargas-Blanco DA, Shell SS. Regulation of mRNA stability during bacterial stress responses. *Frontiers in microbiology*. 2020 Sep 9;11:2111.  
<https://doi.org/10.3389/fmicb.2020.02111>
37. Pizzoccheri R, Falchi FA, Alloni A, Caldarulo M, Camboni T, Zambelli F, Pavesi G, Visentin C, Camilloni C, Sertic S, Briani F. Pathological PNPase variants with altered RNA binding and degradation activity affect the phenotype of bacterial and human cell models. *NAR Molecular Medicine*. 2025 Jan;2(1):ugae028.  
<https://doi.org/10.1093/narmme/ugae028>
38. Singh V, Rai R, Mathew BJ, Chourasia R, Singh AK, Kumar A, Chaurasiya SK. Phospholipase C: underrated players in microbial infections. *Frontiers in Cellular and Infection Microbiology*. 2023 Apr 17;13:1089374.  
<https://doi.org/10.3389/fcimb.2023.1089374>
39. Monturiol-Gross L, Villalta-Romero F, Flores-Díaz M, Alape-Girón A. Bacterial phospholipases C with dual activity: phosphatidylcholinesterase and sphingomyelinase. *FEBS Open Bio*. 2021 Dec;11(12):3262-75.  
<https://doi.org/10.1002/2211-5463.13320>
40. Terehova M, Dzmitruk V, Abashkin V, Kirakosyan G, Ghukasyan G, Bryszewska M, Pedziwiatr-Werbicka E, Ionov M, Gómez R, de La Mata FJ, Mignani S. Comparison of the effects of dendrimer, micelle and silver nanoparticles on phospholipase A2 structure. *Journal of Biotechnology*. 2021 Apr 10;331:48-52.  
<https://doi.org/10.1016/j.jbiotec.2021.03.009>
41. More PR, Pandit S, Filippis AD, Franci G, Mijakovic I, Galdiero M. Silver nanoparticles: bactericidal and mechanistic approach against drug resistant pathogens. *Microorganisms*. 2023 Feb 1;11(2):369.  
<https://doi.org/10.3390/microorganisms11020369>
42. Tsigotaki A, De Geyter J, Šoštaric N, Economou A, Karamanou S. Protein export through the bacterial Sec pathway. *Nature Reviews Microbiology*. 2017 Jan;15(1):21-36.  
<https://doi.org/10.1038/nrmicro.2016.161>
43. Dakal TC, Kumar A, Majumdar RS, Yadav V. Mechanistic basis of antimicrobial actions of silver nanoparticles. *Frontiers in microbiology*. 2016 Nov 16;7:1831.

- <https://doi.org/10.3389/fmicb.2016.01831>
44. Kashyap DR, Rompca A, Gaballa A, Helmann JD, Chan J, Chang CJ, Hozo I, Gupta D, Dziarski R. Peptidoglycan recognition proteins kill bacteria by inducing oxidative, thiol, and metal stress. *PLoS Pathogens*. 2014 Jul 17;10(7):e1004280.  
<https://doi.org/10.1371/journal.ppat.1004280>
  45. Davies O, Mendes P, Smallbone K, Malys N. Characterisation of multiple substrate-specific (d) ITP/(d) XTPase and modelling of deaminated purine nucleotide metabolism. *BMB reports*. 2011;44(11).
  46. Zyryanov AB, Shestakov AS, Lahti R, Baykov AA. Mechanism by which metal cofactors control substrate specificity in pyrophosphatase. *Biochemical Journal*. 2002 Nov 1;367(3):901-6.  
<https://doi.org/10.1042/bj20020880>
  47. Liu W, Worms I, Slaveykova VI. Interaction of silver nanoparticles with antioxidant enzymes. *Environmental Science: Nano*. 2020;7(5):1507-17.  
<https://doi.org/10.1039/C9EN01284B>
  48. Ebbole DJ, Zalkin HT. Cloning and characterization of a 12-gene cluster from *Bacillus subtilis* encoding nine enzymes for de novo purine nucleotide synthesis. *Journal of Biological Chemistry*. 1987 Jun 15;262(17):8274-87.  
[https://doi.org/10.1016/S0021-9258\(18\)47560-6](https://doi.org/10.1016/S0021-9258(18)47560-6)
  49. Saulou-Berion C, Gonzalez I, Enjalbert B, Audinot JN, Fourquaux I, Jamme F, Cocaign-Bousquet M, Mercier-Bonin M, Girbal L. *Escherichia coli* under ionic silver stress: An integrative approach to explore transcriptional, physiological and biochemical responses. *PloS one*. 2015 Dec 22;10(12):e0145748.  
<https://doi.org/10.1371/journal.pone.0145748>
  50. Singh N, Rajwade J, Paknikar KM. Transcriptome analysis of silver nanoparticles treated *Staphylococcus aureus* reveals potential targets for biofilm inhibition. *Colloids and Surfaces B: Biointerfaces*. 2019 Mar 1;175:487-97.  
<https://doi.org/10.1016/j.colsurfb.2018.12.032>
  51. Xia Y, Xie S, Ma X, Wu H, Wang X, Gao X. The *purL* gene of *Bacillus subtilis* is associated with nematicidal activity. *FEMS microbiology letters*. 2011 Sep 1;322(2):99-107.  
<https://doi.org/10.1111/j.1574-6968.2011.02336.x>
  52. Mao BH, Tsai JC, Chen CW, Yan SJ, Wang YJ. Mechanisms of silver nanoparticle-induced toxicity and important role of autophagy. *Nanotoxicology*. 2016 Sep 13;10(8):1021-40.  
<https://doi.org/10.1080/17435390.2016.1189614>
  53. Southworth TW, Guffanti AA, Moir A, Krulwich TA. GerN, an endospore germination protein of *Bacillus cereus*, is a Na<sup>+</sup>/H<sup>+</sup>-K<sup>+</sup> antiporter. *Journal of Bacteriology*. 2001 Oct 15;183(20):5896-903.  
<https://doi.org/10.1128/jb.183.20.5896-5903.2001>
  54. Kawish M, Ullah F, Ali HS, Saifullah S, Ali I, ur Rehman J, Imran M. Bactericidal potentials of silver nanoparticles: novel aspects against multidrug resistance bacteria. *InMetal Nanoparticles for Drug Delivery and Diagnostic Applications*

- 2020 Jan 1 (pp. 175-188). Elsevier.  
<https://doi.org/10.1016/B978-0-12-816960-5.00010-0>
55. Silver S. Bacterial resistances to toxic metal ions-a review. *Gene*. 1996 Jan 1;179(1):9-19
  56. Molina-Hernandez JB, Aceto A, Bucciarelli T, Paludi D, Valbonetti L, Zilli K, Scotti L, Chaves-López C. The membrane depolarization and increase intracellular calcium level produced by silver nanoclusters are responsible for bacterial death. *Scientific Reports*. 2021 Nov 3;11(1):21557.  
<https://doi.org/10.1038/s41598-021-00545-7>
  57. Cao M, Bernat BA, Wang Z, Armstrong RN, Helmann JD. FosB, a cysteine-dependent fosfomycin resistance protein under the control of  $\zeta$ W, an extracytoplasmic-function  $\zeta$  factor in *Bacillus subtilis*. *Journal of bacteriology*. 2001 Apr 1;183(7):2380-3.  
<https://doi.org/10.1128/jb.183.7.2380-2383.2001>
  58. Cameron SJ, Sheng J, Hosseinian F, Willmore WG. Nanoparticle effects on stress response pathways and nanoparticle-protein interactions. *International Journal of Molecular Sciences*. 2022 Jul 19;23(14):7962.  
<https://doi.org/10.3390/ijms23147962>
  59. Helmann JD. Bacillithiol, a new player in bacterial redox homeostasis. *Antioxidants & redox signaling*. 2011 Jul 1;15(1):123-33.  
<https://doi.org/10.1089/ars.2010.3562>
  60. Li YP, Ben Fekih I, Chi Fru E, Moraleda-Munoz A, Li X, Rosen BP, Yoshinaga M, Rensing C. Antimicrobial activity of metals and metalloids. *Annual review of microbiology*. 2021 Oct 8;75(1):175-97.  
<https://doi.org/10.1146/annurev-micro-032921-123231>
  61. Hsueh YH, Lin KS, Ke WJ, Hsieh CT, Chiang CL, Tzou DY, Liu ST. The antimicrobial properties of silver nanoparticles in *Bacillus subtilis* are mediated by released Ag<sup>+</sup> ions. *PloS one*. 2015 Dec 15;10(12):e0144306.  
<https://doi.org/10.1371/journal.pone.0144306>
  62. Handtke S, Albrecht D, Otto A, Becher D, Hecker M, Voigt B. The proteomic response of *Bacillus pumilus* cells to glucose starvation. *Proteomics*. 2018 Jan;18(1):1700109.  
<https://doi.org/10.1002/pmic.201700109>
  63. Ayora S, Carrasco B, Cárdenas PP, César CE, Cañas C, Yadav T, Marchisone C, Alonso JC. Double-strand break repair in bacteria: a view from *Bacillus subtilis*. *FEMS microbiology reviews*. 2011 Nov 1;35(6):1055-81.  
<https://doi.org/10.1111/j.1574-6976.2011.00272.x>
  64. Ezraty B, Gennaris A, Barras F, Collet JF. Oxidative stress, protein damage and repair in bacteria. *Nature Reviews Microbiology*. 2017 Jul;15(7):385-96.  
<https://doi.org/10.1038/nrmicro.2017.26>
  65. Fukui K, Kosaka H, Kuramitsu S, Masui R. Nuclease activity of the MutS homologue MutS2 from *Thermus thermophilus* is confined to the Smr domain. *Nucleic acids research*. 2007 Feb 1;35(3):850-60.  
<https://doi.org/10.1093/nar/gkl735>
  66. Park EN, Mackens-Kiani T, Berhane R, Esser H, Erdenebat C, Burroughs AM, Berninghausen O, Aravind L,

- Beckmann R, Green R, Buskirk AR. *B. subtilis* MutS2 splits stalled ribosomes into subunits without mRNA cleavage. *The EMBO Journal*. 2024 Feb 15;43(4):484-506. <https://doi.org/10.1038/s44318-023-00010-3>
67. Bruna T, Maldonado-Bravo F, Jara P, Caro N. Silver nanoparticles and their antibacterial applications. *International journal of molecular sciences*. 2021 Jul 4;22(13):7202. <https://doi.org/10.3390/ijms22137202>
68. Ayora S, Carrasco B, Cárdenas PP, César CE, Cañas C, Yadav T, Marchisone C, Alonso JC. Double-strand break repair in bacteria: a view from *Bacillus subtilis*. *FEMS microbiology reviews*. 2011 Nov 1;35(6):1055-81. <https://doi.org/10.1111/j.1574-6976.2011.00272.x>
69. Pal A, Bhattacharjee S, Saha J, Sarkar M, Mandal P. Bacterial survival strategies and responses under heavy metal stress: a comprehensive overview. *Critical reviews in microbiology*. 2022 May 4;48(3):327-55. <https://doi.org/10.1080/1040841X.2021.1970512>
70. Maslowska KH, Makiela-Dzbenka K, Fijalkowska IJ. The SOS system: A complex and tightly regulated response to DNA damage. *Environmental and molecular mutagenesis*. 2019 May;60(4):368-84. <https://doi.org/10.1002/em.22267>
71. Stephenson K. Sec-dependent protein translocation across biological membranes: evolutionary conservation of an essential protein transport pathway. *Molecular membrane biology*. 2005 Jan 1;22(1-2):17-28. <https://doi.org/10.1080/09687860500063308>
72. Munir N, Gulzar W, Abideen Z, Hasanuzzaman M, El-Keblawy A, Zhao F. Plant–nanoparticle interactions: Transcriptomic and proteomic insights. *Agronomy*. 2023 Aug 11;13(8):2112. <https://doi.org/10.3390/agronomy13082112>